J MATER RES TECHNOL. 2020;9(5):10291–10304

Available online at www.sciencedirect.com

jmr&t Journal of Materials Research and Technology

https://www.journals.elsevier.com/journal-of-materials-research-and-technology

Original Article

Design and study of a metamaterial based sensor for the application of liquid chemicals detection

Yadgar I. Abdulkarim[a,b], Lianwen Deng[a], Heng Luo[a,*], Shengxiang Huang[a], Muharrem Karaaslan[c], Olcay Altıntaş[c], Mehmet Bakır[d], Fahmi F. Muhammadsharif[e], Halgurd N.Awl[f], Cumali Sabah[g], Khalid Saeed Lateef Al-badri[h]

[a] School of Physics and Electronics, Central South University, Changsha, Hunan 410083, China
[b] Physics Department, College of Science, University of Sulaimani, Sulaimani, 46001, Iraq
[c] Department of Electrical and Electronics, Iskenderun Technical University, Hatay, 31100, Turkey
[d] Department of Computer Engineering Bozok University, Yozgat, 66200, Turkey
[e] Department of Physics, Faculty of Science and Health, Koya University, 44023 Koya, Iraq
[f] Department of Communication Engineering, Sulimani Polytechnic University, Sulaimani, 46001, Iraq
[g] Department of Electrical and Electronics Engineering, Middle East Technical University, Kalkanli, Guzelyurt, 99738, Turkey
[h] Physics Department, University of Samarra, Samarra, 34010, Iraq

ARTICLE INFO

Article history:
Received 2 June 2020
Accepted 9 July 2020
Available online 29 July 2020

Keywords:
Metamaterial
Resonator
Dielectric characteristic
Liquid detection

ABSTRACT

The detection of chemical samples having close dielectric response is a big challenge as the detection principle is driven by the variations in the dielectric parameters of the investigated samples. In the current work, a new metamaterial-based sensor is designed and fabricated in order to be used for the detection of liquid chemicals in the frequency range from 8 to 12 GHz. Several designs were tested using genetic algorithm, which is embedded in the CST microwave studio, in order to optimize the desired dimensions of the resonator. The simulation and experimental results showed that the proposed sensor is working well to detect various liquids, including (i) clean and waste transformer oils, (ii) corn, cotton and olive oils, (iii) branded and unbranded diesels and (iv) aniline doped ethyl-alcohol and benzene doped carbon tetrachloride. This was made possible through the occurrence of a shift in the resonant frequency of about 250 MHz, 200 MHz, 250 MHz, 150 MHz and 50 MHz for the aforementioned samples, respectively. The sensing mechanism was interpreted through the surface current and electric field distributions. We believe that the proposed sensor is viable to be used in various applications including liquid chemicals detection and industrial applications.

* *Corresponding author.*
E-mail: luohengcsu@csu.edu.cn (H. Luo).

https://doi.org/10.1016/j.jmrt.2020.07.034

1. Introduction

Metamaterials (MTMs) are well known for their singular and periodic structure which is able to show a negative permittivity and permeability [1]. The physical properties of MTMs are largely dependent on the shape, design, orientation and dimensions of their constituted unit cells. MTM has found itself in various applications including biosensors [2–5], antennas [6,7], signal absorbers [8,9], energy harvesting [10,11] and microwave lenses [12,13]. Split ring resonators (SRR) are the most commonly used topology of MTMs due to its practical shape and adaptability for various applications. Different interesting designs and architectures can be made possible with the help of simulation tools such as finite integration technique (FIT) and finite element methods (FEM) to improve the sensitivity of MTM sensors. The principle of MTM sensors for the detection of materials is based on the shift in resonant frequency. This is resulted from capacitance changes due to the strong coupling effect taking place when the sample, with a specific dielectric constant, is inserted into the sensing area [14]. A microstrip SRR based chemical sensor was presented in 2012 aiming at identifying methanol and ethanol solvents at operating frequency of 1.9 GHz [15]. Another SRR based sensor printed on FR4 substrate was reported to show the possible application of MTM sensor that is by employing a WR90 waveguide between 8 GHz and 12 GHz [16]. Furthermore, an open SRR coupled with a microfluidic channel was proposed for the sensing application of isopropanol, methanol and glucose D [17]. Another SRR based MTM sensor was studied by Velez et al., in which microfluidic channels were used to define the real time shifts in resonant frequency, thereby detecting ethanol and deionized water [18]. In order to prevent errors caused from positioning and realizing a fully integrated microfluidic sensor, Awang et al. designed another MTM sensor, by which a 60 MHz shift in the resonant frequency was realized [19] and Sadeqi et al. proposed a flexible MTM sensor in 2017 [20]. MTM inspired microfluidic sensor can also be realized by combining the desired MTM absorbers [21–24]. MTM absorber based chemical sensors are generally printed on a FR4 material, which can be used to define ingredients of chemicals based on the principle of variations in the dielectric constant [25,26].

Researchers proposed various approaches to increase the quality factor of these sensors by means of printing the sensors on low loss dielectric substrates [27,28], designing different shapes of resonators [29–32]. However, there is yet a great tendency in developing unique metamaterial sensors for wide applications [33,34]. We have previously reported different MTMs based sensors integrated with transmission lines in order to detect the branded and unbranded diesels [35,36]. To the best of our knowledge, there is no reported sensor in literature which has been specifically developed to detect liquid chemicals having almost similar dielectric responses. The main issue arises here is that due to the close dielectric values of branded and unbranded chemicals, it would be quite difficult for the conventional and low sensitive MTM based sensors to them. This is because the working principle of the sensors is based on variations in the dielectric parameters of the samples under test.

A metamaterial absorber based on G-shaped resonator was reported aiming at boosting the quality factor of the absorber in S-band region without considering its optimization and application in X-band region [37]. In the current work, a new G-shaped metamaterial sensor is designed, optimized and fabricated so as to be utilized for the detection of various oils and liquid chemicals such as transformer oil, corn oil, cotton oil, olive oils, diesels, aniline doped ethyl alcohol and benzene doped carbon tetrachloride in the X-band frequency region. Compared to the previous works [38,39], in the current study parametric analysis is also performed on various substrates in order to choose the optimum dimension for the sensor. As such, the sensor is well tuned to show any possible shifts in the resonant frequency despite the existence of trivial changes in the dielectric constant of the samples. Furthermore, the proposed structure is cheap and stable in operation which is compatible to be operated over a wide range of frequencies from 1 to 20 GHz. We believe that the proposed sensor is viable to be used in various applications including liquid chemicals detection and industrial applications.

2. Structure design and simulation

The proposed MTM sensor is presented in Fig. 1. Full-wave finite integration technique (FIT) based on high-frequency electromagnetic solver, CST microwave studio was used for the numerical analysis. The MTM sensor is composed of three main layers. The bottom layer, having a thickness of 10 mm, is the sensor reservoir used to hold the samples under test. The middle layer is Flame Retardant 4 (FR-4) dielectric substrate, which was chosen due to its low loss, high mechanical strength and low cost. Its relative permittivity is 4.3 with loss tangent of 0.02 and thickness of 1.6 mm. The top layer made of resonators was deposited on the front and back side of the FR-4 substrate. The resonators are made of copper metal with conductivity of 5.8×10^7 S/m and thickness of 35 μm. Fig. 1(a) shows the dimension of the unit cell which is compatible for X-band waveguide and it is in consistence with the experimental analysis. The overall size of the structure is 22.86×10.16 mm^2. The sensor was designed to be operated in the X-band region due to easy access and production of a sensitive structure having compatible sample holder in the X-band range of frequency. Taking into consideration the dielectric constant of the sensible materials and the frequency range in which a possible resonant shifting is happened, several designs were investigated through parametric study and the use of genetic algorithm in order to optimize the desired dimensions of the resonator in the X-band region. Table 1 shows the featured dimensions of the resonator used in the current study. The CST microwave studio includes an optimization technique which is based on genetic algorithm (GA) approach. The GA was utilized to optimize the required dimensions of the resonator. Genetic algorithm is a stochastic search method working on the principles of natural genetic systems. It performs a search to provide the best possible solution for fitness function of an optimization problem [40,41].

In the simulation process, different boundary conditions are allowed to be applied aiming at achieving the waveguide measurements for the proposed structure with effective

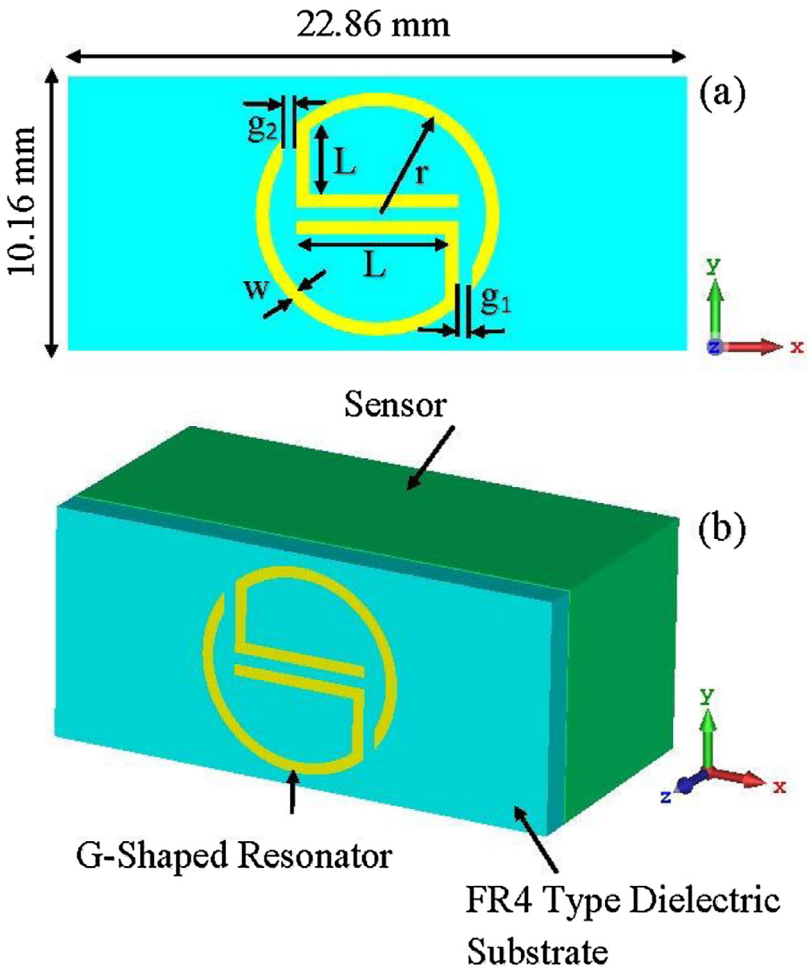

Fig. 1 – The proposed metamaterial-based liquid sensor: (a) design dimensions and (b) perspective view.

Table 1 – The dimension parameters of the proposed resonator.

Parameters	Value (mm)
L_1	6
L_2	3.1
r	4
g_1	0.5
g_2	0.5
w	0.5

dimensions. Taking the boundary conditions into consideration, including free space, periodic distribution, PEC/PMC and PEC, are acceptable due to the metallic nature of the side-wall waveguide. As such, for the measurement of S-parameters by using WR-90 waveguide along with a compatible sample holder, the boundary condition of perfect electrical conductor (PEC) was assigned at the x- and y-directions, while the z-axis was assumed to be open (added space) alongside the propagation direction, as shown in Fig. 2.

In order to understand the sensor principle and its governing electrical mechanism, an equivalent circuit diagram for the proposed structure was presented by using resistor (R), inductor (L) and capacitor (C), as shown in Fig. 3(b). The resonator can be represented by a total resistance (Rt) inductance

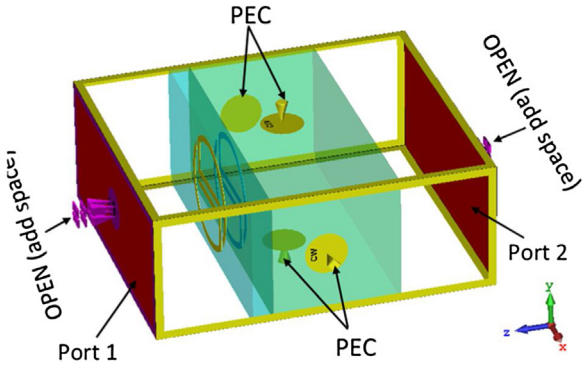

Fig. 2 – MTM based liquid sensor design: boundary conditions and added port of each side of the proposed structure in the simulation program.

(Lt) and capacitance (Ct). The resonator has two similar gaps denoted by Cg. Hence, the proposed resonator can behave like an RLC model. The capacitance of the sensor layer (Cs) placed on the backside of the structure can be attenuated with liquid samples having different electrical properties.

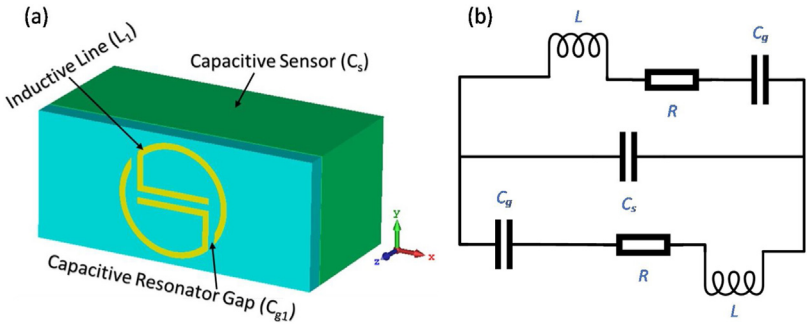

Fig. 3 – a) Design of the inductive and capacitive parts of the proposed structure and (b) equivalent circuit diagram of the proposed metamaterial-based senor.

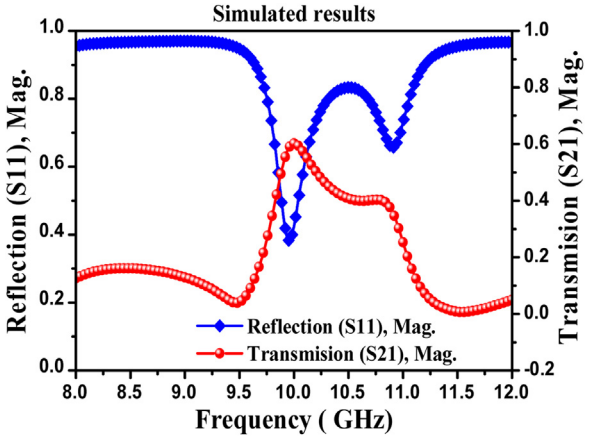

Fig. 4 – Reflection spectra and transmission spectra for the metamaterial-based sensor without chemicals liquids.

The equation below shows the value of capacitance of the sensor layer,

$$Cs = (4A - g)Cpul \quad (1)$$

Where, g and A are the value of split gap and average dimension of the resonator. Cpul is capacitance per unit length which can be calculated as [42],

$$C_{pul} = \sqrt{\varepsilon_r}/c_0 Z_0 \quad (2)$$

Where, Z_0 is the characteristic impedance of the line and C_0 is the velocity of the light in free space. Hence, the total capacitance (Ct) of the overall structure can be represented by,

$$Ct = Co + Cg + Cs \quad (3)$$

Where Co is the capacitance effect of the surrounding space, Cg is the split/gap capacitors and C_S is the capacitance effect of the sample placed inside the sensor layer. CS value can vary for different samples due to differences in the complex permittivity characteristics which can be expressed by

$$\varepsilon_{sample} = \varepsilon'_{sample} + \varepsilon''_{sample} \quad (4)$$

Hence, the impedance of the split ring resonator can be defined as,

$$Z_r = R_t + j\omega L_t + \frac{1}{j\omega C_t} \quad (5)$$

Where, Zr, Rt, j and ω are respectively denoting the total impedance, total resistance of the split ring resonator, imaginary unit and angular frequency.

The resonance frequency of the proposed structure can be calculated by using this equation

$$f_0 = \frac{1}{2\pi\sqrt{L_t C_t}} \quad (6)$$

Where L_t the total inductance value of the structure. It is clear that the resonance frequency of resonator is inversely proportional to the overall inductance and capacitance of the proposed resonator. Therefore, these two parameter play a major role in defining the sensor sensitivity. It can be noted that the fundamental operation of the sensor structure is related to the interaction between the sensor layer and the resonator.

3. Numerical and experimental studies of the proposed sensor for various liquids

In this section, a numerical investigation is performed on the proposed resonator to be used for sensing various liquids in the X-band frequency range using the Finite Integration Technique (FIT) based high-frequency electromagnetic solver CST microwave studio. The important parts of the proposed structure are the resonators which are placed at the front and back side of the FR4 dielectric substrate. The sensor layer was designated as a reservoir of 10 mm thick to be filled by the liquids, where the magnetic field of the transmitted electromagnetic wave is perpendicularly exposed to it in the z direction. In the numerical study and experimental testing, two waveguide ports, namely port 1 and port 2 were connected to the

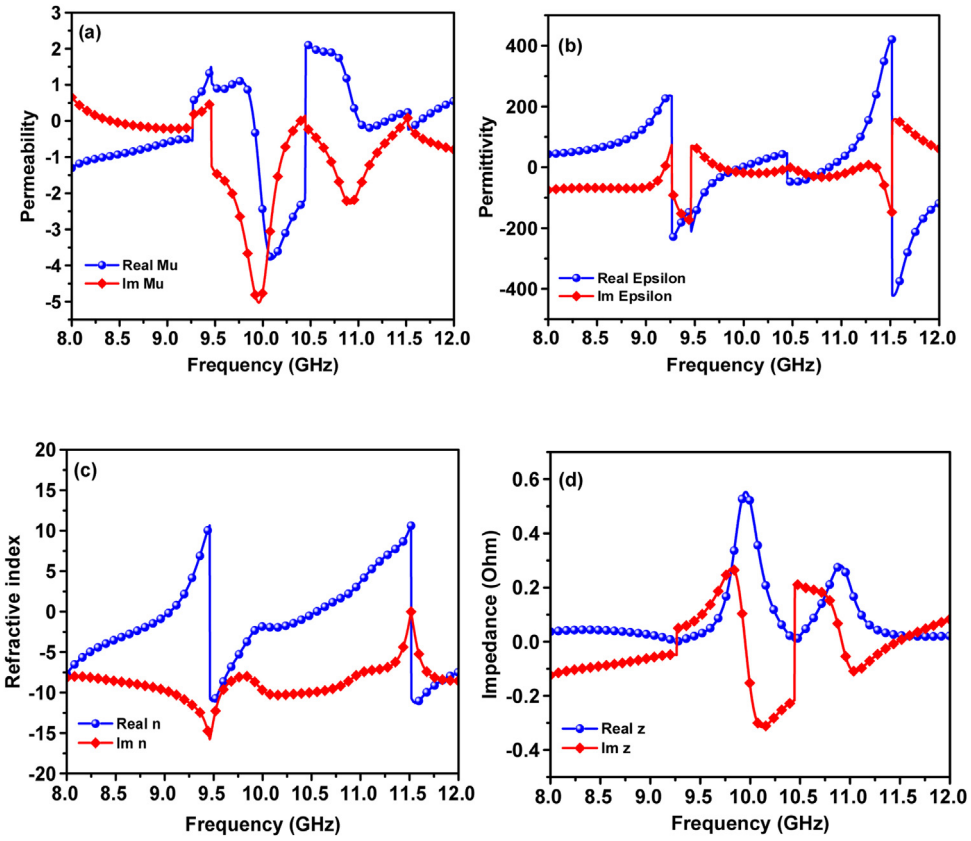

Fig. 5 – Simulated physical parameters of the proposed MTM based sensor: (a) effective permeability, (b) effective permittivity, (c) refractive index and (d) impedance.

front and back side of the proposed structure for monitoring the transmission coefficient (S_{21}). The size of the structure is determined for X-band waveguide dimensions at the frequency range of 8–12 GHz. The value of reflection coefficient (S_{11}) and transmission coefficient (S_{21}) has been carried out when there are no liquids in the sensor layer, as shown in Fig. 4. It can be seen from the figure that the reflection and transmission coefficients presented a maxima and minima at approximately 9.95 GHz which corresponds to the X-band frequency range. This result demonstrating that the proposed metamaterials based sensor structure can be effectively utilized to distinguish various liquids when they are placed in the sensor layer and the sensor is operated in the X-band frequency. As such, different lubricant samples, with electrically sensible characteristics, have been chosen to be investigated both numerically and experimentally in the desired frequency range.

To reveal the MTM property of the proposed sensor, the real and imaginary parts of effective permeability (μ), permittivity (ε), refractive index (n) and impedance (z) of the sensor were extracted, as shown in Fig. 5(a–d).

These parameters were determined based on the following equations [43]:

$$\mu = nz \tag{7}$$

$$\varepsilon = \frac{n}{z} \tag{8}$$

Where the impedance (z) and refractive index (n) term in Eqs. (7) and (8) are obtained from the Eqs. (9) and (10), as follows:

$$z = \pm\sqrt{\frac{(1+S_{11})^2 - S_{21}^2}{(1-S_{11})^2 - S_{21}^2}} \tag{9}$$

$$n = \frac{1}{k_0 d}\left[\left[\ln\left(e^{ink_0d}\right)\right]'' - i\left[\ln\left(e^{ink_0d}\right)\right]'\right] \tag{10}$$

Where S_{21} and S_{11} in Eq. (9) denotes the transmission and reflection coefficients of the MTM based sensor. The exponential term in Eq. (10) is represented by $e^{ink_0d} = \frac{S_{21}}{1-S_{11}\frac{z-1}{z+1}}$, where $[\ln(e^{ink_0d})]'$ represents the real component, $[\ln(e^{ink_0d})]''$ denotes the imaginary component of the complex number, k_0 denotes the wave-number and d represents the maximum length of the unit cell. Here, the complete resonator is considered as a single unit cell.

One can notice from Fig. 5 that negative values for permeability and permittivity are obtained in the frequency range from 8 GHz to 10.50 GHz, which defines the presence of MTM behavior by the proposed sensor.

However, beyond the frequency limit of 10.50 GHz, the value of permeability grows higher such that $\mu > 1$. This high permeability characteristic of the proposed MTM based sensor is used to realize the compactness.

In order to understand the operating mechanism of the proposed metamaterial sensor, surface current and electric field

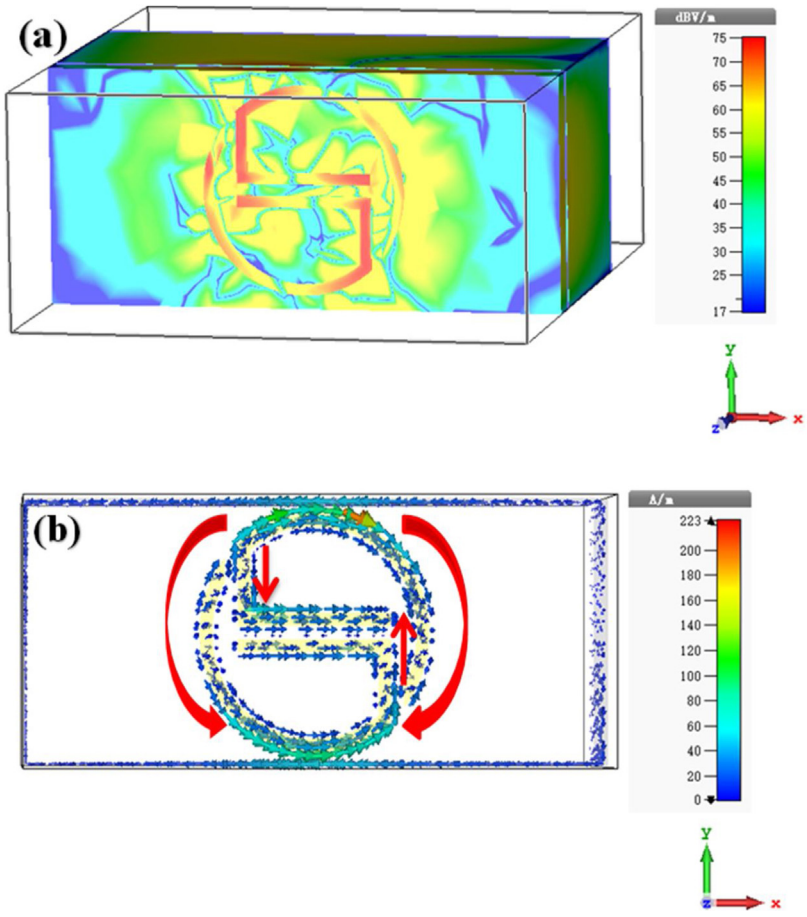

Fig. 6 – Simulated result for the proposed sensor structure: (a) electric field distribution and (b) surface current distribution.

distributions were investigated, as shown in Fig. 6. The distributions were obtained at the resonance frequency of 10 GHz for the case of empty sensor layer. Once can notice from Fig. 6 (a) that the electric filed intensity is mostly concentrated at the resonator in the upper and lower parts of the resonator, especially at the capacitive parts of the resonator. Hence, the proposed structure is able to sense any small changes in the electrical characteristics of the sample placed in the sensor layer.

The simulated surface current distribution at the resonance frequency of 10 GHz is shown in Fig. 6(b). Noteworthy, the surface current is highly localized at the upper and lower arcs of the resonator in the clockwise and anti-clockwise directions, respectively. Furthermore, parallel and anti-parallel currents are distributed at the left and right arms of the resonator, thereby controlling the electric and magnetic response, respectively. The simulated surface current distribution for the proposed structure is an obvious indication for the presence of a resonance phenomenon due to the electric dipole.

In order to show the operating principle and characterization of the proposed device, the sensor layer is assumed to be filled with air. Fig. 7 shows the impact of varying design parameters of the resonator on the resonant frequency. The resonant frequency of the proposed sensor was seen to be mainly dependent on the width (w), radius (r), and length (L) of the resonator. Results showed that when the width (w) of the resonator was increased from 0.1 mm to 0.9 mm, the resonant frequency was decreased from 9.55 GHz to 9.28 GHz, as shown in Fig. 7(a). The general trend of this variation was found to be inversely proportional.

Noticeably, the most influential parameter on the resonant frequency was seen to be the radius of the resonator. When the radius was increased from 3.6 mm to 4.4 mm, the resonant frequency was gradually decreased from 9.75 GHz to 8.75 GHz, as shown in Fig. 7(b). However, the least influential parameter was the length (L_1) of the resonator. Fig. 7(c) shows that when the length is increased from 5.2 mm to 6.8 mm, the resonant frequency is hardly decreased. This can be ascribed to the fact that the surface current and electric field are weakly distributed along the arm length (L_1) of the resonator, which is in agreement with the observations made in Fig. 6. The resonant frequency shift can be explained based on the general resonance formula, $1/2\pi\sqrt{LC}$. Since capacitance is directly proportional to the permittivity of the sample, any increase in the dielectric parameter of the sample is resulted in the increased effective capacitance of the resonator. Hence, enlarged capacitance is led to decrease in the resonant frequency of the system [15].

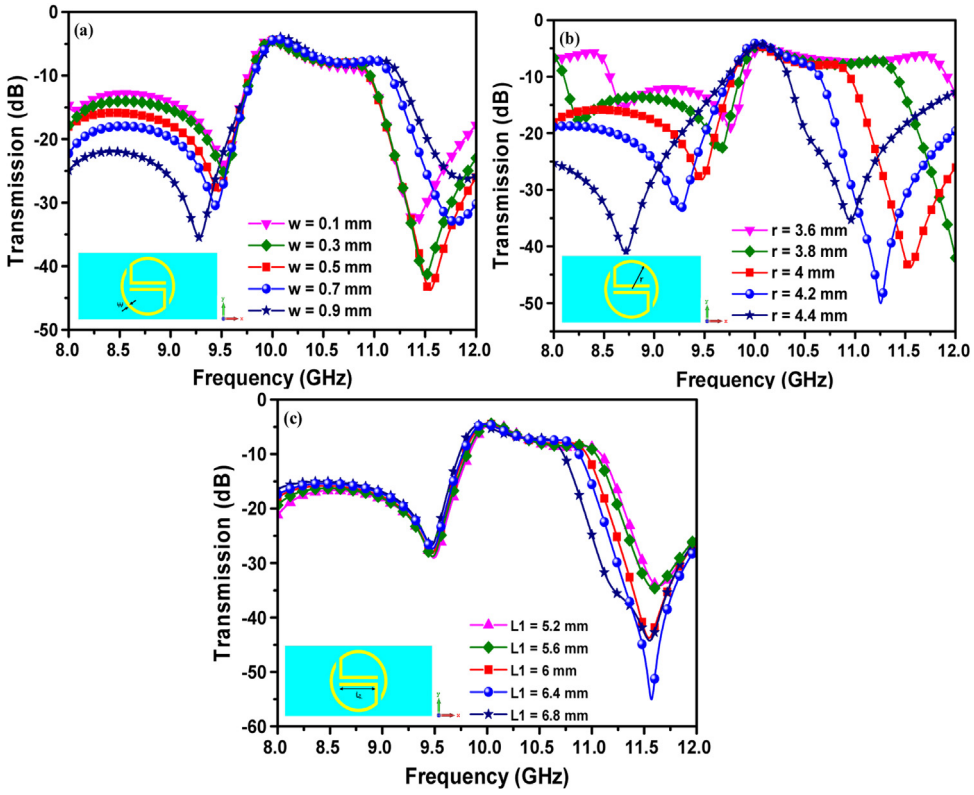

Fig. 7 – Effect of the variation of (a) width (w), (b) Radius (r) and (c) Length (L_1) of the resonator on the transmission spectrum peaks of the proposed MTM based sensor.

We conclude that the dimensional aspects of the resonator are the main factors affecting the overall performance of the proposed metamaterials-based sensor. Hence, their values need to be aimfully tuned.

Following the simulation results, experimental investigations were also carried out, whereby the proposed sensor structure was fabricated by using the LPKF ProtoMAT E33 prototyping machine Computerized Numerical Control (CNC) with FR4 dielectric substrate on the top of sensor layer. The sensor layer has a thickness of 10 mm, while the copper material resonator has been placed on both front and backside of the FR4 substrate. The simulation and experimental measurements were taken in the same condition.

The fabricated sensor structure is depicted in Fig. 8(a). Experimental studies were arranged in the X-band waveguide in front of the sample holder. The two waveguide, WR90 and sample holder are illustrated in Fig. 8 (b). The sample holder depth was 10 mm, which was filled with the liquid samples. It was placed at the front side of the waveguide, where the face of the sample holder was tied by a captain band and its back was coated by a thin copper band.

After fabricating the proposed sensor, the designed structure was coupled to the waveguide adaptor and the measurement was recorded by using Agilent PNA-L series vector network analyzer (VNA) in the frequency range from 10 MHz to 43.5 GHz, as shown in Fig. 8(c). The VNA was calibrated by using a special calibration kit with open circuit, short circuit and 50-Ohm load connectors for the two ports. Before taking the measurements, the frequency in the VNA was assigned in the X-band between 8–12 GHz. It is expected that calibration errors along with the cable defects and manufacturer imperfection are reasons for the occurrence of practical mismatch.

Furthermore, the electrical properties of each liquid samples were studied by using an open ended coaxial probe. The dielectric constant and dielectric loss factor were measured by immerging 85070E dielectric probe kit that is by connecting it to a vector network analyzer (VNA), as shown in Fig. 9. The dielectric probe was calibrated by using air and pure water with known electromagnetic properties in the same frequency range adapted for the study and at room temperature (25°). For this purpose, a special short circuit kit was used via a proper software program inside the VNA. Then, the dielectric characteristics of the liquid samples have been obtained in the desired frequency range.

Following the experimental setup, we measured the transmission coefficient (S_{21}) with the presence of liquid sample holder, waveguide, adaptor and sensor structure, as shown in Fig. 8. First, the sample to be studied was injected into the sample holder and then the transmission coefficient (S_{21}) was measured in the desired frequency range from 8–12 GHz. The same measurement procedure was repeated for each sample.

The transmission coefficient (S_{21}) was calculated numerically in the CST Microwave studio software by importing the dielectric properties of each selected samples into the program, while the sensing characteristics of the proposed structure was measured by placing the samples into the sensor layer.

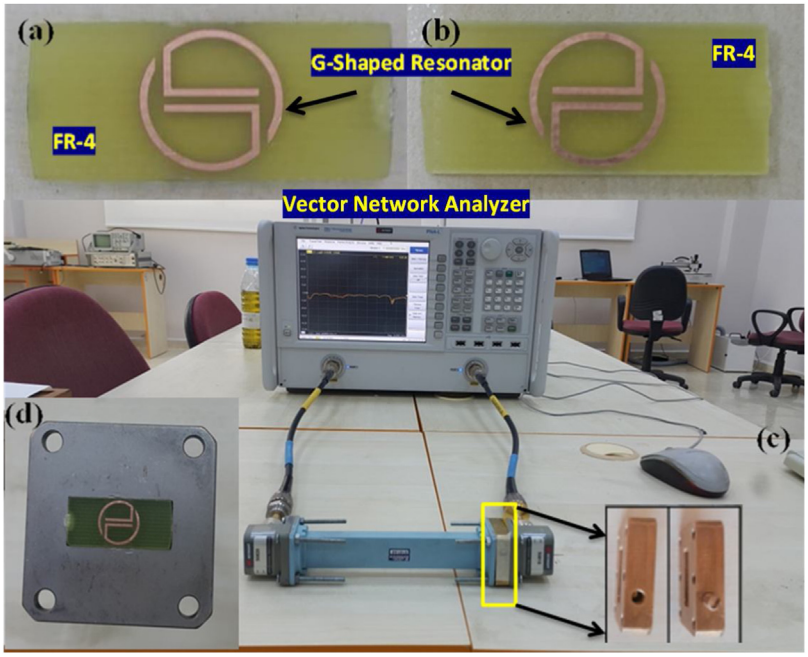

Fig. 8 – (a) Front view of the fabricated metamaterial based sensor, (b) back view, (c) experimental setup with waveguide configuration and (d) Sample holder-captain band with manufactured sample.

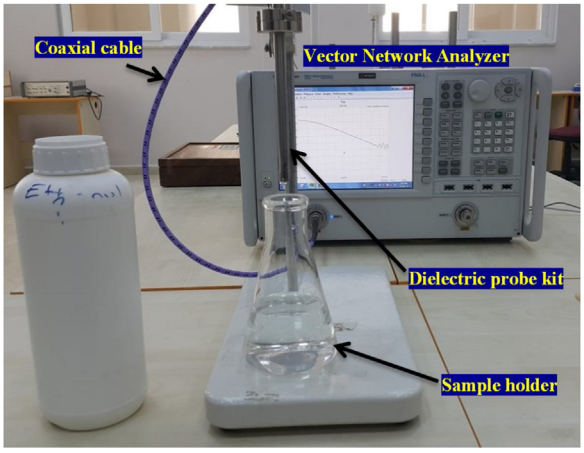

Fig. 9 – Experimental setup to determine the relative permittivity measurement of the samples using 85070E dielectric probe kit.

3.1. *Study on the detection of transformer oil condition*

In this part, numerical and experimental studies were performed to investigate the transformer oil condition through analyzing the changes that might be happened in the X-band frequency range. The use of transformer oil can perform at least four functions in a transformer. The oil serves as an insulator, cools the transformer and extinguishes other discharges. In addition, gases arising from the oxidation of oil, moisture and gases from the breakdown of cellulose insulation, as well as gases and moisture from the atmosphere, dissolve in the oil. Careful monitoring of the gases dissolved in the oil, as well as other properties of the oil, provides the most accurate information on the condition of the transformer. Therefore, this part of the work was mainly focused on the determination of the transformer oil condition, either to be clean or waste oil. The dielectric constant and dielectric lose results of the clean and waste transformer oils at 8–12 GHz are shown in Fig. 10. It was found that the dielectric constant is about 2.84 and 2.73 for the clean and waste transformer oils, respectively. The dielectric loss value of the clean and waste transformer oils were obtained to be about 0.151 and 0.16, respectively.

In addition to the differences noticed in the dielectric properties of the clean and waste samples, which can be relied on for differentiating the samples, the proposed sensor was utilized to address the wave transmission behavior of the device upon the presence of the samples. Simulation and experimental investigations on the clean and waste oil using the proposed metamaterials sensor at 8–12 GHz are shown in Fig. 11. One can notice that the proposed sensor is well capable of distinguishing the two samples based on the transmission information fetched at the high resonance frequency of about 11.3 GHz. Both simulation and experimental results have clearly showed this shift in the transmission coefficient such that the waste oil sample provided larger absolute values of the transmission coefficient at the resonant frequency.

3.2. *Study on the detection of herbal oil samples*

Each type of oil can have a unique quality based on its ingredients and physical conditions. We anticipate that the electrical properties of the oils can be used as a viable tool for quality control investigations and understanding their scores in health benefits. In this section, we measured the dielectric properties of corn, olive and cotton oils by using dielectric probe kit at X-band, as shown in Fig. 9. The dielectric permit-

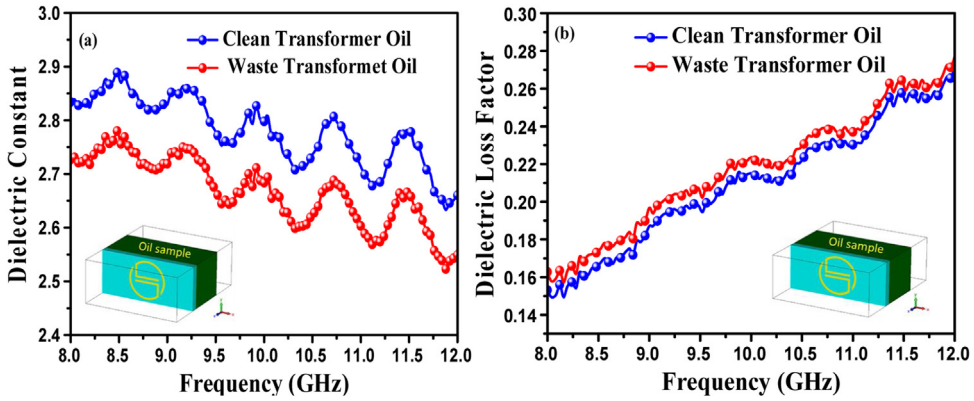

Fig. 10 – Measured results for the clean and waste oil samples: (a) the dielectric constant and (b) dielectric loss factor in X-band frequency.

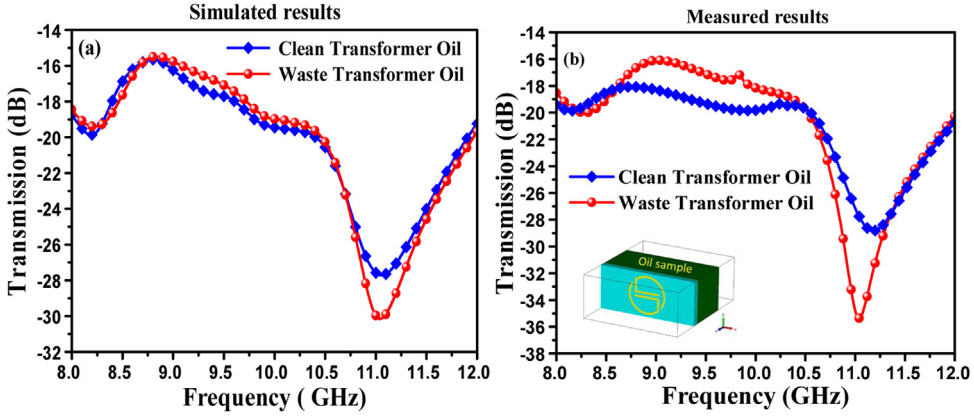

Fig. 11 – (a) Simulation and (b) experimental transmission behavior with the presence of the clean and waste transformer oils at frequency 8–12 GHz.

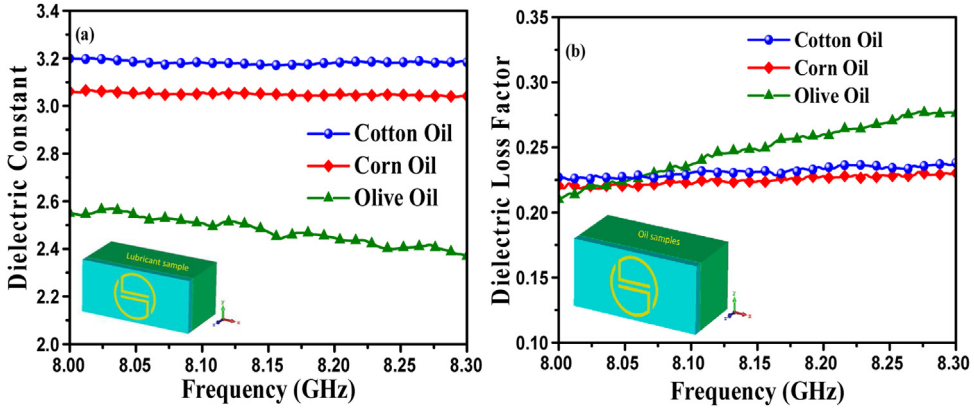

Fig. 12 – (a) The dielectric constant and (b) dielectric loss factor measurement results for the corn, cotton and olive oils at X-band.

tivity and dielectric loss factor were recorded and results are shown in Fig. 12(a) and (b), respectively. The value of dielectric constant for cotton, corn and olive oil are 3.2, 3.08 and 2.55, respectively. The dielectric loss factor was measured to be 0.202, 0.205 and 0.226 for the olive, corn and cotton oils, respectively. It is however that these values are close to each other at 8 GHz, yet the proposed metamaterial structure has precisely detected the samples.

It is seen from Fig. 13 that results of simulation and experimental transmission coefficients for the oil samples in X-band frequency regime are relatively different. This can be ascribed to the errors arise due to calibration, instrument

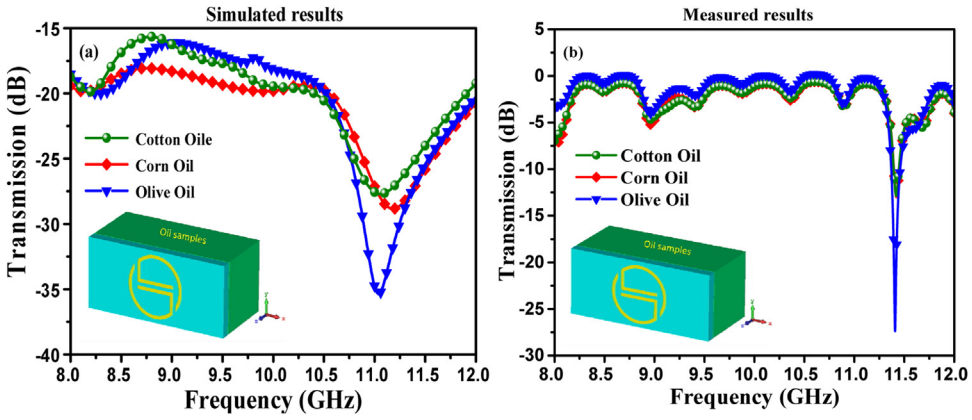

Fig. 13 – (a) Simulation and (b) experimental results for the corn, cotton and olive oils at frequency 8–12 GHz.

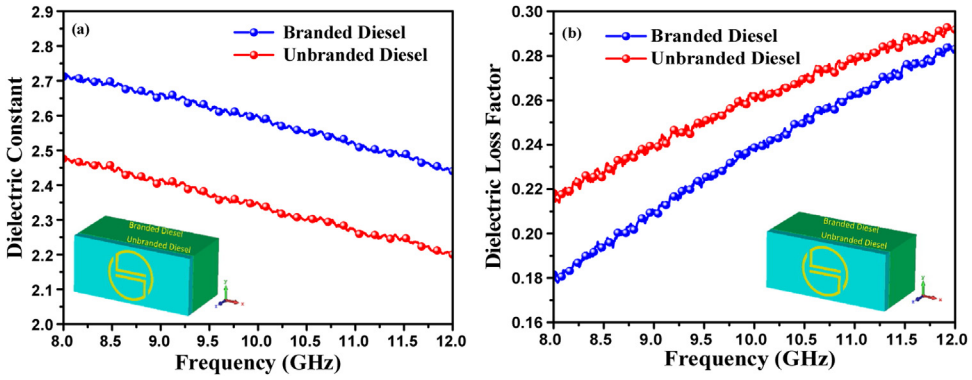

Fig. 14 – (a) The dielectric constant and (b) dielectric loss factor for the branded and unbranded diesel samples in 8–12 GHz.

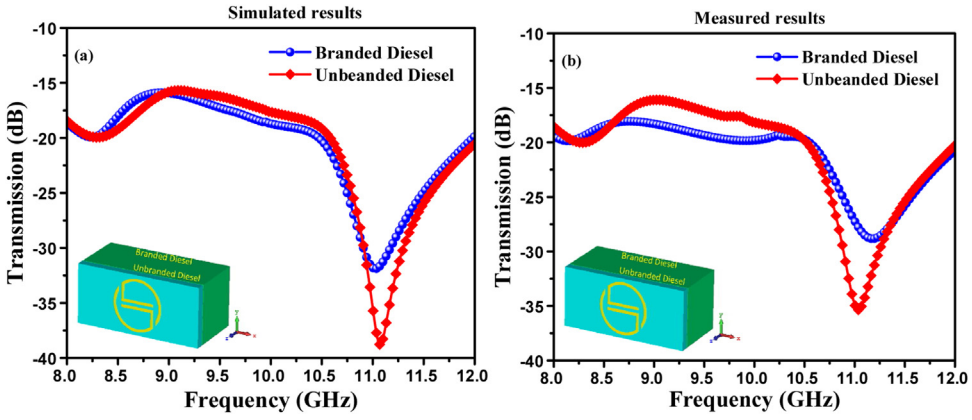

Fig. 15 – Sensing results for the branded and unbranded diesel samples in 8–12 GHz (a) Simulated result and (b) Experimental result.

and mismatched fabrication. In the numerical studies, the obtained result for the transmission coefficient of olive oil was minimum at about 11 GHz, while this was at 11.20 GHz and 11.25 GHz for the corn oil and cotton oil, respectively. Besides, the transmission coefficient was at different values for each of the oil samples when they are measured experimentally and estimated numerically. These results implying that the proposed structure can precisely detect various types of liquids despite the closed value of their dielectric behavior.

3.3. *Study of branded and unbranded diesel*

In South Asian countries, fuel adulteration is a global danger associated with the engine performance decline, environmental pollution and governmental tax loss. There have been several works performed in literature for the fuel adulteration detection using fiber grating technology, density measurement method, gas chromatography and dielectric probe kit method [44–47]. The detection of the branded and unbranded diesel is crucial for the government custom, the health of the

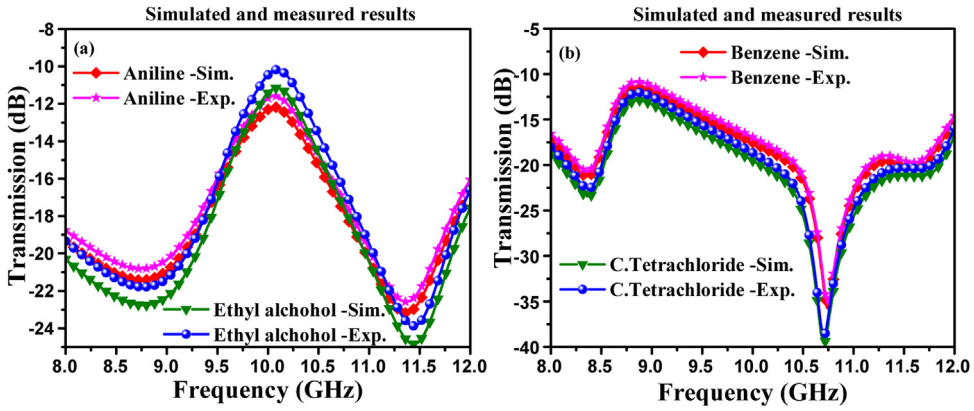

Fig. 16 – Numerical and experimental sensing results for (a) aniline and ethyl-alcohol samples and (b) for the benzene and carbon-tetrachloride samples in 8–12 GHz.

Table 2 – Sensitivity comparison of the proposed sensor to those reported in literature.

Reference	Material	Dielectric Constant	Frequency Range (GHz)	Resonant Frequency Shift (MHz)
[34]	waste transformer oil	2.5 for clean transformer oil and 2.51	8–12	61
[35]	Clean oil and waste oil	2.74 for clean oil and 2.87 waste oil	1–8	63
[36]	Branded and unbranded diesel	2.71 for branded diesel and 2.48 for unbranded diesel	80–12	60
[38]	Clear and dirty transformer oil	3 for clear transformer oil and 2.75 for dirty transformer oil	8–12	70
[39]	Clean and waste transformer oil	2.7 for clean transformer oil and 2.81 for waste transformer oil	4–5	40
[47]	Olive oil, cotton oil	2.54 for olive oil and 2.88 for 40% cotton oil with 60% olive oil	8–12	150
This work	Clean and dirty transformer oil	2.84 for clean transformer oil and 2.73 for waste transformer oil	8–12	250
This work	Branded and unbranded diesel	2.71 for branded diesel and 2.48 for unbranded diesel	8–12	250
This work	Olive oil and cotton oil.	3.2 for olive oil and 2.55 for cotton oil	8–12	200

user and diesel motor engine is highly depending on the purity of fuel. The disadvantages of the mentioned methods for fuel adulteration are large size and being expensive. In this work, we propose a highly sensitive and cost effective technique, which is based on metamaterials sensor in order to distinguish the branded and unbranded diesels.

The electrical properties of the branded and unbranded diesel were first measured by using the dielectric probe kit and the test results for the dielectric constant are shown in Fig. 14. The measurement was obtained in the X-band frequency regime. It was seen from the results that the dielectric constant value of the branded diesel sample starts from 2.71 at 8 GHz and ends to 2.43 at 12 GHz. The dielectric constant values of the unbranded diesel are 2.48 at 8 GHz and 2.15 at 12 GHz. The tangent value of the branded diesel sample starts from 0.48 at 8 GHz and ends to 0.7 at 12 GHz. The tangent value of the unbranded diesel was found to be 0.53 at 8 GHz and equals 0.64 at 12 GHz.

It is worth noting that the proposed sensor can be effectively utilized to detect various qualities of diesel, as shown in Fig. 15. From the simulated results for instance, the unbranded diesel sample presented at higher resonance frequency around 11.12 GHz have deeper transmission coefficient compared to that of the branded one in Fig. 15 (a). The value of the transmission coefficient is about −32 dB and −38.75 dB for the branded and unbranded diesel respectively. In order to support the simulated results we investigated the experimental study as shown in Fig. 15 (b) the value of transmission coefficient is about 28.75 dB and 35.5 dB for the branded and unbranded diesel respectively. Noticed the numerical and experimental study is a good agreement with each other and both results showed the metamaterials based sensor can easily detect different kinds for diesel.

3.4. *Study on the detection of liquid chemicals*

The final experiment was to perform detection of chemical liquids namely aniline, ethyl-alcohol, benzene and carbon-tetrachloride in the frequency range 8–12 GHz, the measured value of the dielectric constant and dielectric loss factor for the aniline, ethyl-alcohol, benzene and carbon-tetrachloride are 5.809044, 5.781161, 2.56916, 2.522, 0.15583, 0.145451, 0.080846 and 0.079589 respectively. As shown in Fig. 16. The simulated results showed that transmission coefficient has lower level at 11.30 GHz for aniline compared to that of ethyl-alcohol at 11.5 GHz. The resulted frequency shift was seen to be about 200 MHz. The experimental study has been demonstrated to compare the simulated results as depicted in Fig. 16(a) the resonance shift was monitored to be around 120 MHz, both numerical and experimental results are good agreement. Furthermore the minimum transmission coefficient was recorded for the benzene and carbon tetrachloride samples and it was happened at about 10.75 GHz and 10.70 GHz, respectively. This was also accompanied with a frequency shift of 50 MHz According to these results, the proposed metamaterial based sensor can easily detect chemical liquids by using microwave technique without any chemical analysis. The structure can be used for different industrial and electrochemical sensing applications.

The proposed metamaterials-based sensor compared to other works published in literatures in term of frequency range, dielectric constant, sensitivity and years of published, the results are shown in Table 2. The quality factor can be used to show tangible results. The best quality factor has been observed during benzene simulation and experimental study, as shown in Fig. 16b. The quality factor was found to be as high as 300. Comparably, this value is higher than those reported in literature [39–47].

4. Conclusion

A resonator was successfully designed and fabricated in order to be used for the detection of liquid chemicals in the X-band frequency region. It was concluded that the proposed sensor has easily differentiated the clean transformer oil from the waste one by means of a 250 MHz shift in the resonant frequency despite close values of the dielectric constant of about 2.84 and 2.73 for the clean and waste transformer oils, respectively. It was found that the dielectric constant for cotton, corn and olive oils is 3.2, 3.08 and 2.55, respectively, while the resonant frequency shift was noticed to be about 200 MHz. Furthermore, the measured value of dielectric constant for the branded and unbranded diesels was found to be 2.71 and 2.48, respectively. Concluding, the proposed sensor is well adapted to detect liquid chemicals, for instance the shift in resonant frequency between the branded and unbranded diesels was about 250 MHz, while that for the aniline doped ethyl-alcohol and benzene doped carbon-tetrachloride was 150 MHz and 50 MHz, respectively. The experimental results were seen to be in a good agreement with the simulation ones. The sensor structure was successfully designed for the real-time, fast, low cost, durable, and accurate detection of the samples. We believe that our proposed sensor can be highly interested for many applications of industrial, liquid chemicals and medicine.

Funding

This work was supported by the National Key Research and Development Program of China (Grant no. 2017YFA0204600), the National Natural Science Foundation of China (Grant no. 51802352) and the Fundamental Research Funds for the Central Universities of Central South University (Grant no. 2018zzts355).

Conflicts of interest

The authors declare no conflict of interest.

CRediT authorship contribution statement

Yadgar I. Abdulkarim: Conceptualization, Methodology, Software, Formal analysis, Investigation, Data curation, Writing - original draft, Visualization, Project administration. **Lianwen Deng:** Project administration, Funding acquisition. **Pin Zhang:** Supervision. **Heng Luo:** Writing - review & editing. **Shengxiang Huang:** Writing - review & editing. **Muharrem Karaaslan:** Conceptualization, Validation, Supervision, Resources, Project administration. **Olcay Altıntaş:** Methodology, Validation. **Mehmet Bakır:** Methodology, Writing - original draft. **Fahmi F. Muhammadsharif:** Validation, Resources, Visualization, Writing - review & editing. **Halgurd N.Awl:** Software, Formal analysis, Data curation, Visualization. **Cumali Sabah:** Validation. **Khalid Saeed Lateef Al-badri:** Writing - review & editing.

Acknowledgments

The author would like to thanks for Central South University and Iskenderun Technical University for the technical supports.

REFERENCES

[1] Shelby RA, Smith DR, Schultz S. Experimental verification of a negative index of refraction. Science 2001;292:77–9, http://dx.doi.org/10.1126/science.1058847.
[2] Withayachumnankul W, Jaruwongrungsee K, Fumeaux C, Abbott D. Metamaterial-inspired multichannel thin-film sensor. IEEE Sens J 2012;12:1455–8.
[3] Aristov AI, Manousidaki M, Danilov A, Terzaki K, Fotakis C, Farsari M, et al. 3D plasmatic crystal metamaterials for ultra-sensitive bio sensing. Sci Rep 2016;6:1–8.
[4] Afapour ZOV, Ajati YAH, Ajati MOH. Graphene-based mid-infrared biosensor. J Opt Soc Am B 2017;34:2586–92.
[5] Bakir M. Electromagnetic-based microfluidic sensor applications. J Electrochem Soc 2017;164:B488–94.
[6] Johnson MC, Brunton SL, Kundtz NB, Kutz JN. Sidelobe canceling for reconfigurable holographic metamaterial antenna. IEEE Trans Antennas Propag 2015;63(4):1881–6.

[7] Nasimuddin N, Chen ZN, Qing X. Bandwidth enhancement of a single-feed circularly polarized antenna using a metasurface: metamaterial-based wideband CP rectangular microstrip antenna. IEEE Antennas Propag Mag 2016;58(2):39–46.
[8] Bağmancı M, Karaaslan M, Altıntaş O, Karadağ F, Tetik E, Bakır M. Wideband metamaterial absorber based on crrs with lumped elements for microwave energy harvesting. J Microw Power Electromagn Energy 2018;52(1):45–59.
[9] Bakır M, Karaaslan M, Unal E, Akgol O, Sabah C. Microwave metamaterial absorber for sensing applications. Opto-Electron Rev 2017;25(4):318–25.
[10] Bakır M, Karaaslan M, Altıntaş O, Bagmancı M, Akdogan V, Temurtaş F. Tunable energy harvesting on UHF bands especially for GSM frequencies. Int J Microw Wirel Technol 2018;10(1):67–76.
[11] Bağmancı M, Karaaslan M, Unal E, Özaktürk M, Akgol O, Karadağ F, et al. Wide band fractal-based perfect energy absorber and power harvester. Int J Rf Microw Comput Eng 2019;29(7):e21597.
[12] Qi MQ, Tang WX, Ma HF, Pan BC, Tao Z, Sun YZ, et al. Suppressing side-lobe radiations of horn antenna by loading metamaterial lens. Sci Rep 2015;5:9113.
[13] Mukherjee S, Su Z, Udpa L, Udpa S, Tamburrino A. Enhancement of microwave imaging using a metamaterial Lens. IEEE Sens J 2019;19(13):4962–71.
[14] Salim A, Lim S. Review of recent metamaterial microfluidic sensors. Sensors (Basel) 2018;18(1):232, http://dx.doi.org/10.3390/s18010232.
[15] Withayachumnankul W, Jaruwongrungsee K, Tuantranont A, Fumeaux C, Abbott D. Metamaterial-based microfluidic sensor for dielectric characterization. Sens Actuators A Phys 2013;189:233–7, http://dx.doi.org/10.1016/j.sna.2012.10.027.
[16] Kim HK, Yoo M, Lim S. Novel ethanol chemical sensor using microfluidic metamaterial. In: Proceedings of the IEEE International Symposium on Antennas and Propagation & USN National Radio Science Meeting. 2015. p. 1358–9.
[17] Byford JA, Park KY, Chahal P. Metamaterial inspired periodic structure used for microfluidic sensing. In: Proceedings of the Electronic Components Technology Conference; San Diego. 2015. p. 1997–2002.
[18] Velez P, Su L, Grenier K, Mata-Contreras J, Dubuc D, Martin F. Microwave microfluidic sensor based on a microstrip splitter/combiner configuration and split ring Resonators (SRRs) for dielectric characterization of liquids. IEEE Sens J 2017;17:6589–98, http://dx.doi.org/10.1109/JSEN.2017.2747764.
[19] Awang RA, Tovar-Lopez FJ, Baum T, Sriram S, Rowe WST. Meta-atom microfluidic sensor for measurement of dielectric properties of liquids. J Appl Phys 2017;121, http://dx.doi.org/10.1063/1.4978012.
[20] Sadeqi A, Sonkusale S. Low-cost metamaterial-on-paper chemical sensor. Transducers Int Conf Solid-State Sens Actuators Microsyst 2017;25:1437–40, http://dx.doi.org/10.1109/TRANSDUCERS.2017.7994329.
[21] Nguyen TT, Lim S. Wide incidence angle-insensitive metamaterial absorber for both TE and TM polarization using eight-circular-sector. Sci Rep 2017;7:1–11, http://dx.doi.org/10.1038/s41598-017-03591-2.
[22] Lee D, Jeong H, Lim S. Electronically switchable broadband metamaterial absorber. Sci Rep 2017;7:1–10, http://dx.doi.org/10.1038/s41598-017-05330-z.
[23] Kim HK, Lee D, Lim S. A fluidically tunable metasurface absorber for flexible large-scale wireless ethanol sensor applications. Sensors 2016;16:1246, http://dx.doi.org/10.3390/s16081246.
[24] Bakir M, Karaaslan M, Akgol O, Altintas O, Unal E, Sabah C. Sensory applications of resonator based metamaterial absorber. Optik 2018;168:741–6.
[25] Abdulkarim YI, Deng L, Karaaslan M, Unal E. Determination of the liquid chemicals depending on the electrical characteristics by using metamaterial absorber based sensor. Chem Phys Lett 2019;732:136655.
[26] Abdulkarim YI, Deng L, Altintas O, Unal E, Karaaslan M. Metamaterial absorber sensor design by incorporating swastika shaped resonator to determination of the liquid chemicals depending on electrical characteristics. Physica E Low Dimens Syst Nanostruct 2019:113593.
[27] Wang Wudeng, Zheng Li, Xiong Li, Qi Jianguang, Li Baoying. High Q-factor multiple Fano resonances for high-sensitivity sensing in all-dielectric metamaterials. OSA Continuum 2019;2:2818–25.
[28] Xie Q, Dong GX, Wang BX, Huang WQ. High-q fano resonance in terahertz frequency based on an asymmetric metamaterial resonator. Nanoscale Res Lett 2018;13(1):294, http://dx.doi.org/10.1186/s11671-018-2677-0.
[29] Bakir M, Delihacioglu K, Karaaslan M, Dincer F, Sabah C. U-shaped frequency selective surfaces for single-and dual-band applications together with absorber and sensor configurations. IET Microw Antennas Propag 2016;10(3):293–300.
[30] Chuma EL, Iano Y, Fontgalland G, Roger LLB, Loschi H. PCB-integrated non-destructive microwave sensor for liquid dielectric spectroscopy based on planar metamaterial resonator. Sens Actuators A Phys 2020:112112.
[31] Chuma EL, Iano Y, Fontgalland G, Roger LLB. Microwave sensor for liquid dielectric characterization based on metamaterial complementary split ring resonator. IEEE Sens J 2018;18(24):9978–83.
[32] Hoque A, Tariqul Islam M, Almutairi A, Alam T, Jit Singh M, Amin N. A polarization independent Quasi-TEM metamaterial absorber for X and ku band sensing applications. Sensors 2018;18(12):4209.
[33] Abdulkarim YI, Deng L, Karaaslan M, Unal E. Determination of the liquid chemicals depending on the electrical characteristics by using metamaterial absorber based sensor. Chem Phys Lett 2019;732:136655.
[34] Altıntaş O, Aksoy M, Ünal E. Design of a metamaterial inspired omega shaped resonator based sensor for industrial implementations. Physica E Low Dimens Syst Nanostruct 2019:113734.
[35] Abdulkarim Yadgar I, Deng Lianwen, Karaaslan Muharrem, Altıntaş Olcay, Awl Halgurd N, Muhammadsharif Fahmi F, et al. Novel metamaterials-based hypersensitized liquid sensor integrating omega-shaped resonator with microstrip transmission line. Sensors 2020;20:943, http://dx.doi.org/10.3390/s20030943.
[36] Tamera Ahmet, Karadağa Faruk, Ünala Emin, Abdulkarim Yadgar I, Deng Lianwen, Altintasa Olcay, et al. Metamaterial based sensor integrating transmission line for detection of branded and unbranded diesel fuel. Chem Phys Lett 2020;742:137169, http://dx.doi.org/10.1016/j.cplett.2020.137169.
[37] Al-Badri KSL. Very high Q-Factor based on G-Shaped resonator type metamaterial absorber. Ibn AL-Haitham J Pure Appl Sci 2018:159–66.
[38] Bakır M, Karaaslan M, Karadag F, Dalgac S, Ünal E, Akgöl O. Metamaterial sensor for transformer oil, and microfluidics. Appl Comput Electromagn Soc J 2019;34(5).
[39] Altintaş O, Aksoy M, Ünal E, Karaaslan M. Chemical liquid and transformer oil condition sensor based on metamaterial-inspired labyrinth resonator. J Electrochem Soc 2019;166(6):B482–8.
[40] Hameed SS, Muhammad FF, Hassan R, Saeed F. Gene selection and classification in microarray datasets using a hybrid approach of PCC-BPSO/GA with multi classifiers. J Comput Sci 2018;14(6):868–80.

[41] Nguyen TD, Duroc Y, Vu VY, Vuong TP. Genetic algorithm for optimization of L-shaped PIFA antennas. Int J Microw Wirel Technol 2011;3(06):691–9, http://dx.doi.org/10.1017/s1759078711000985.
[42] Saha C, Siddiqui JY, Antar YM. Square split ring resonator backed coplanar waveguide for filter applications. In: General Assembly and Scientific Symposium, 2011 XXXth URSI. 2011. p. 1.
[43] Chen X, Grzegorczyk TM, Wu B-I, Pacheco Jr J, Kong JA. Robust method to retrieve the constitutive effective parameters of metamaterials. Phys Rev E 2004;70:016608, http://dx.doi.org/10.1103/physreve.70.016608.
[44] De Moutusi, Pathak Akhilesh Kumar, Singh Vinod Kumar. Single channel photonic crystal fiber based high sensitive petrol adulteration detection sensor. Optik 2019;183:539–46, http://dx.doi.org/10.1016/j.ijleo.2019.03.001.
[45] Leghrib Radouane, Ouacha El Houssaine, Zouida Ahmed, Faiz Bouazza, Amghar Abdallah. Monitoring automobile fuel adulteration using ultrasound technique for environmental issues. Measurement 2020;150:107004, http://dx.doi.org/10.1016/j.
[46] Vempatapu Bhanu Prasad, Tripathi Deependra, Kumar Jagdish, Kanaujia Pankaj K. Determination of kerosene as an adulterant in diesel through chromatography and high-resolution mass spectrometry. SN applied Science 2019;1:614, http://dx.doi.org/10.1007/s42452-019-0637-7.
[47] Bakır Mehmet, Dalgaç Sekip, Karaaslan Muharrem, Karadağ Faruk, Unal Oğuzhan Akgo Emin, Depçi Tolga, et al. A comprehensive study on fuel adulteration sensing by using triple ring resonator type metamaterial. J Electrochem Soc 2019;166(12):B1044–52, http://dx.doi.org/10.1149/2.1491912jes.